

Thermoelectric effects in quantum dots

M.Yoshida^{a,*}; L.N. Oliveira^b

^a*Unesp-Universidade Estadual Paulista, Departamento de Física, IGCE-Rio Claro, Brazil*

^b*Instituto de Física de São Carlos, USP, Brazil*

Abstract

We report a numerical renormalization-group study of the thermoelectric effect in the single-electron transistor (SET) and side-coupled geometries. As expected, the computed thermal conductance and thermopower curves show signatures of the Kondo effect and of Fano interference. The thermopower curves are also affected by particle-hole asymmetry.

Key words: Kondo effect, Fano interference, thermopower, numerical renormalization-group

PACS: 72.15.Qm, 73.23.Hk, 73.50.Lw

1 Introduction

The transport properties of mesoscopic devices are markedly affected by electronic correlations. Gate potentials applied to such devices give experimental control over effects once accessible only in special arrangements. In particular, the Kondo effect and Fano anti-resonances have been unequivocally identified in the conductance of single-electron transistors (SET) [1,2,3]; of Aharonov-Bohm rings [4]; and of quantum wires with side-coupled quantum dots [5]. Another achievement was a recent study of the thermopower, a quantity sensitive to particle-hole asymmetry that monitors the flux of spin entropy [6]. This work presents a numerical renormalization-group study [10,11,12] of the thermoelectric properties of nanodevices. We consider a quantum dot coupled to conduction electrons in the two most widely studied geometries: the single-electron transistor (SET), in which the quantum dot bridges two-dimensional

* Instituto de Geociências e Ciências Exatas de Rio Claro, UNESP, Brazil
Email address: myoshida@rc.unesp.br (M.Yoshida).

gases coupled to electrodes; and the T -shaped device, in which a quantum dot is side-coupled to a quantum wire.

2 Thermoelectric properties

Thermoelectric properties are traditionally studied in two arrangements: the Seebeck (open circuit) and Peltier (closed circuit) setups [13]. In the former, the steady-state electric current vanishes. A temperature gradient drives electrons towards the coldest region, and induces an electric potential difference between the hot and the cold extremes. The expression $S = -\Delta V/\Delta T$, where ΔV is the potential difference induced by the temperature difference ΔT , then determines the thermopower S . Since the electrons transport heat, the heat current Q can also be measured, and the thermal conductance κ can be obtained from the relation $Q = -\kappa\nabla T$.

In the Peltier setup, a current J is driven through a circuit kept at uniform temperature. The heat flux $Q = \Pi J$ is then measured and determines the Peltier coefficient Π , which is proportional to the thermopower: $\Pi = ST$.

We prefer the Seebeck setup. The transport coefficients are then computed from the integrals [7]

$$I_n(T) = -\frac{2}{h} \int_{-D}^{+D} \varepsilon^n \frac{\partial f(\varepsilon)}{\partial \varepsilon} \mathcal{T}(\varepsilon, T) d\varepsilon \quad (n = 0, 1, 2). \quad (1)$$

where $\mathcal{T}(\varepsilon, T)$ is the transmission probability at energy ε and temperature T , $f(\varepsilon)$ is the Fermi distribution and D is the half width of the conduction band. The electric conductance G , the thermopower S , and the thermal conductance κ are given by [7]

$$G = e^2 I_0(T) \quad (2)$$

$$S = -\frac{I_1(T)}{eT I_0(T)} \quad (3)$$

$$\kappa = \frac{1}{T} \left\{ I_2(T) - \frac{I_1^2(T)}{I_0(T)} \right\}, \quad (4)$$

respectively. Our problem, therefore, is to compute $\mathcal{T}(\varepsilon, T)$ for a correlated quantum dot coupled to a gas of non-interacting electrons.

3 Thermal Conductance and Thermopower of a SET

Recent experiments [3] have detected Fano anti-resonances in coexistence with the Kondo effect in SETs. The interference indicates that the electrons can flow through the dot or tunnel directly from one electrode to the other. The transport properties of the SET can be studied by a modified Anderson model [9,14], which in standard notation is described by the Hamiltonian

$$H = \sum_{k,\alpha} \varepsilon_k c_{k,\alpha}^\dagger c_{k,\alpha} + t \sum_{k,k'} (c_{k,L}^\dagger c_{k,R} + H.c.) + V \sum_{\bar{k},\alpha} (c_{\bar{k},\alpha}^\dagger c_d + H.c.) + H_d. \quad (5)$$

Here the quantum-dot Hamiltonian is $H_d = \varepsilon_d c_d^\dagger c_d + U n_{d,\uparrow} n_{d,\downarrow}$, with a dot energy ε_d , controlled by a gate potential applied to the dot, that competes with the Coulomb repulsion U . The summation index α on the right-hand side takes the values L and R , for the left and right electrodes respectively. The tunneling amplitude t allows transitions between the electrodes, while V couples the electrodes to the quantum dot. The Hamiltonian (5) being invariant under inversion, it is convenient to substitute even (+) and odd (−) operators $c_{k\pm} = (c_{kR} \pm c_{kL})/\sqrt{2}$ for the c_{kL} and c_{kR} . It results that only the c_{k+} are coupled to the quantum dot. For brevity, we define the shorthand $\gamma \equiv \pi \rho t$, where ρ is the density of conduction states; and the dot-level width $\Gamma \equiv \pi \rho V^2$.

In the absence of magnetic fields, the transmission probability through the SET is [8,9]

$$\mathcal{T}(\varepsilon, T) = T_0 + \frac{4\Gamma\sqrt{T_0 R_0}}{1 + \gamma^2} \Re\{G_{d,d}\}(\varepsilon, T) + \frac{2\Gamma(T_0 - R_0)}{1 + \gamma^2} \Im\{G_{d,d}\}(\varepsilon, T),$$

where $G_{dd}(\varepsilon, T)$ is the retarded Green's function for the dot orbital, and we have defined $T_0 \equiv 4\gamma^2/(1 + \gamma^2)^2$ and $R_0 \equiv 1 - T_0$.

To compute \mathcal{T} , we rely on the numerical-renormalization group (NRG) diagonalization of the model Hamiltonian [10]. Although the resulting eigenvectors and eigenvalues yield essentially exact results for $\Im\{G_{dd}\}(\varepsilon, T)$, the direct computation of $\Re\{G_{dd}\}$ is unwieldy. We have found it more convenient to define the Fermi operator

$$b \equiv \left(\frac{2\Gamma}{1 + \gamma^2}\right)^{1/2} c_d + \left(\frac{4\gamma^2}{1 + \gamma^2}\right)^{1/2} \frac{1}{\sqrt{\pi\rho}} \sum_k c_{k+}, \quad (6)$$

because the imaginary part of its retarded Green's function $G_{bb}(\varepsilon, T)$ is directly related to the transmission probability: aided by the two equations of

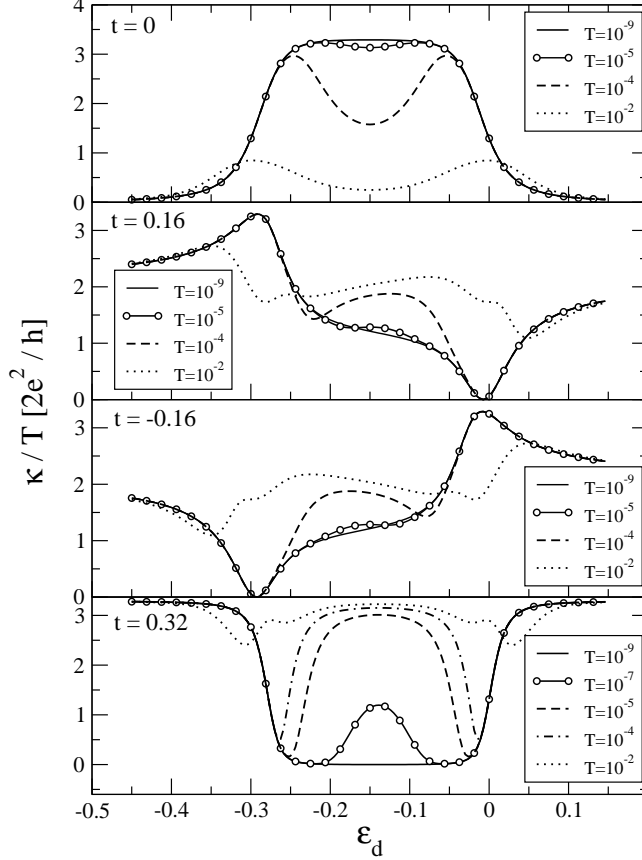


Fig. 1. Thermal conductance κ , normalized by the temperature T , as a function of the dot energy for $U = 0.3D$ and four t s, at the indicated temperatures. The top panel, with $t = 0$, shows no sign of interference. The second (third) panel, with $t = 0.16D$ ($t = -0.16D$) displays a Fano antiresonance. In the bottom panel, $t = 0.32D$, the conductance vanishes in the Kondo valley as $T \rightarrow 0$.

motion relating $G_{kk'}$ to G_{dk} , and G_{kd} to G_{dd} , straightforward manipulation of Eq. (6) show that $\mathcal{T}(\varepsilon, T) = -\Im\{G_{b,b}\}(\varepsilon, T)$. In practice, we (i) diagonalize H iteratively [10]; (ii) for each pair of resulting eigenstates ($|m\rangle, |n\rangle$), compute the matrix elements $\langle m|b_\sigma|n\rangle$; (iii) thermal average the results [15,16] to obtain $\Im\{G_{b,b}\}(\varepsilon, T)$; (iv) substitute the result for $\mathcal{T}(\varepsilon, T)$ in Eq. (1); and (v) evaluate the integral for $n = 0, 1, 2$ to obtain $I_n(T)$ ($n = 0, 1, 2$).

Figure 1 shows numerical results for the thermal conductance as a function of the gate energy ε_d . Well above or well below the Kondo temperature T_K , we expect the thermal and electric conductances to obey the Wiedemann-Franz law $\kappa/T = \pi^2 G/3$ and hence show the thermal conductance normalized by the temperature T . Each panel represents a tunneling parameter t and displays the thermal-conductance profile for the indicated temperatures. All curves were computed for $\Gamma = 10^{-2}D$, and $U = 0.3D$.

The top panel shows the standard SET, with no direct tunneling channel. At the lowest temperature ($k_B T = 10^{-9}D$), the model Hamiltonian close to

the strong-coupling fixed point, the Kondo screening makes the quantum dot transparent to electrons, so that in the Kondo regime [$\Gamma \ll \min(|\varepsilon_d|, 2\varepsilon_d + U)$] the Wiedemann-Franz law pushes the ratio $3\kappa/\pi^2T$ to the unitary limit $2e^2/h$. At higher temperatures, the Kondo cloud evaporates and the thermal conductance drops steeply. The maxima near $\varepsilon_d = 0$ and $\varepsilon_d = -U$ reflect the two resonances associated with the transitions $c_d^1 \leftrightarrow c_d^0$ and $c_d^1 \leftrightarrow c_d^2$.

In the next two panels, the direct tunneling amplitude substantially increased, the current through the dot tends to interfere with the current bypassing the dot. To show that a particle-hole transformation is equivalent to changing the sign of the amplitude t , we compare the curves with $t = 0.16D$ (second panel) with $t = -0.16D$ (third panel). At low temperatures, in the former (latter) case, the interference between the $c_d^1 \leftrightarrow c_d^0$ and $c_d^1 \leftrightarrow c_d^2$ transitions is constructive near $\varepsilon_d = 0$ ($\varepsilon_d = -U$) and destructive near $\varepsilon_d = U$ ($\varepsilon_d = 0$). At intermediate dot energies, $\varepsilon_d \approx -U/2$, the amplitudes for direct transition and for transition through the dot have orthogonal phases and fail to interfere, so that the resulting current is the sum of the two individual currents.

In the bottom panel, the direct tunneling amplitude t is dominant. For gate potentials disfavoring the formation of a dot moment, heat flows from one electrode to the other. In the Kondo regime, however, at low temperatures, the Kondo cloud coupling the dot to the electrode orbitals closest to it blocks transport between the electrodes. As the Kondo cloud evaporates, the thermal conductance in the $\varepsilon_d \approx -U/2$ rises with temperature, so that the resulting profile is symmetric to the one in the top panel. The two resonances near $\varepsilon_d = 0$ and $\varepsilon_d = -U$, which are independent of Kondo screening, keep the thermal conductance low even at relatively high temperatures.

Figure 2 shows thermopower profiles for the same amplitudes t discussed in Fig. 1. In contrast with the thermal conductance, the thermopower is sensitive to particle-hole asymmetry: heat currents due to holes (electrons) make it positive (negative). For the standard SET ($t = 0$, top panel), the thermopower is negligible at low temperatures and vanishes at the particle-hole symmetric parametrical point $\varepsilon_d = -U/2$.

With $|t| = 0.16D$, particle-hole symmetry is broken at $\varepsilon_d = -U/2$, and temperatures comparable to T_K make the thermopower sizeable in the Kondo regime. For $t = 0.16D$, the sensitivity to particle-hole asymmetry makes the interference between electron (hole) currents constructive (destructive) for both $\varepsilon_d = 0$ and for $\varepsilon_d = U$, while for $t = -0.16D$ it is destructive (constructive).

For $t = 0.32D$, direct tunneling again dominant, in the Kondo regime ($\varepsilon_d \approx -U/2$) the thermopower becomes sensitive to the Kondo effect, which is chiefly due to electrons (holes) above (below) the Fermi level. The thermopower therefore emerges as a probe of direct-tunneling leaks in SETs, one that may help

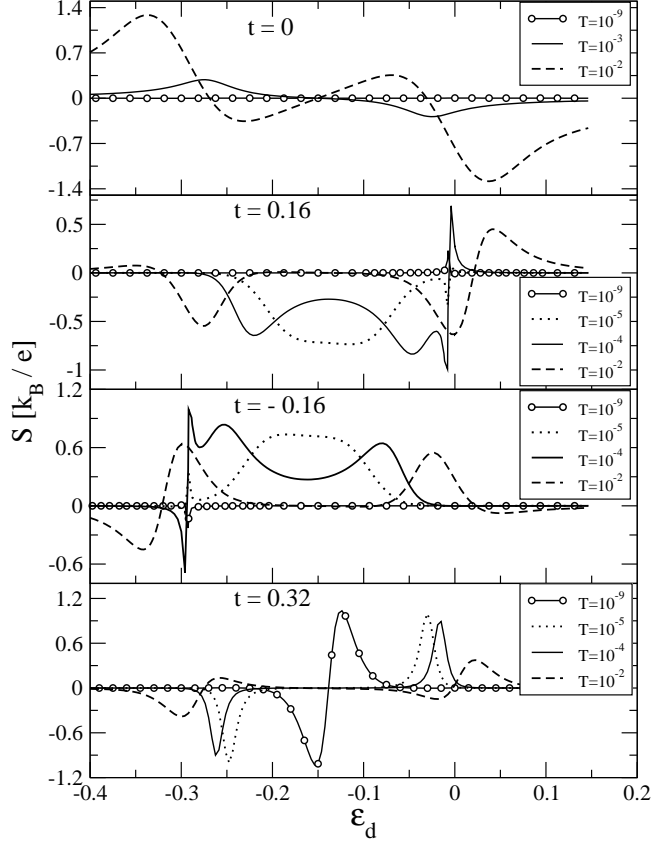


Fig. 2. Thermopower as a function of ε_d for the four tunneling amplitudes t in Fig. 1. Again $\Gamma = 0.01D$ and $U = 0.3D$. For each t , the profile of the thermal power is presented at the indicated temperatures.

identify the source of interference in this and other nanodevices.

4 Side-coupled quantum dot

We have also studied the T -shaped device, in which the dot is side-coupled to the wire [5]. Again, we considered the Seebeck setup. The quantum wire now shunting the two electrodes, we drop the coupling proportional to t on the right-hand side of Eq. (5) and employ the standard Anderson Hamiltonian

$$H_s = \sum_k \varepsilon_k c_k^\dagger c_k + V \sum_k (c_{k,\sigma}^\dagger c_d + H.c.) + H_d \quad (7)$$

where $H_d = \varepsilon_d c_d^\dagger c_d + U n_{d,\uparrow} n_{d,\downarrow}$ is the dot Hamiltonian. The transmission probability is now given by $\mathcal{T}(\varepsilon, T) = 1 + \pi \rho V^2 \Im\{G_{d,d}\}(\varepsilon, T)$ where $G_{d,d}(\varepsilon, T)$. Following the procedure outlined above, we have diagonalized the Hamiltonian H_s iteratively and computed the electrical conductance, the thermal conduc-

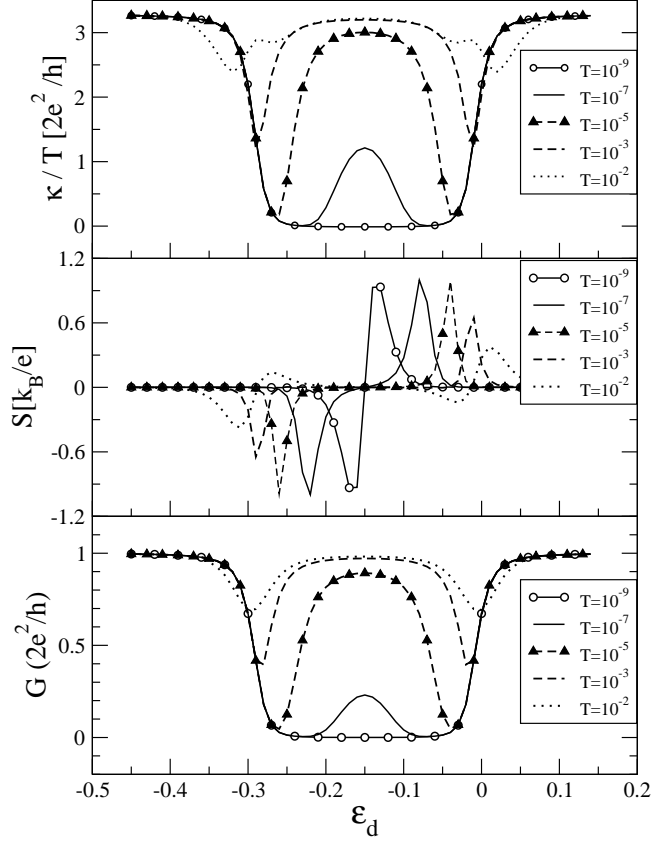


Fig. 3. The thermal conductance, thermopower and electric conductance are presented as a function of ε_d . The temperature dependence of each quantity is also presented.

tance and the thermopower as functions of the gate potential ε_d . Figure 3 displays results for $U = 0.3D$, and $\Gamma = 0.01D$.

Not surprisingly—the wire is equivalent to a large tunneling amplitude, i. e., to $t \sim D$ —the transport coefficients mimic those of the $t = 0.32D$ SET. At low temperatures ($T \ll T_K$) in the Kondo regime, for instance, the Kondo cloud blocks transport through the wire segment closest to the dot. The thermal and electrical conductances thus vanish for $\varepsilon_d \approx -U/2$. As the temperature rises, the evaporation of the Kondo cloud allows transport and both conductances rise near the particle-hole symmetric point. At low temperatures, the sensitivity to particle-hole asymmetry enhances the thermopower in the Kondo regime, a behavior analogous to the bottom panel in Fig. 2.

5 Conclusions

We have calculated the transport coefficients for the SET and the side-coupled geometries. In both cases, the thermal dependence and the gate-voltage pro-

files show signatures of the Kondo effect and of quantum interference. Our essentially exact NRG results identify trends that can aid the interpretation of experimental results. In the side-coupled geometry, in particular, the Kondo cloud has marked effects upon the thermopower.

6 Acknowledgments

Financial support by the FAPESP and the CNPq is acknowledged.

References

- [1] D. Goldhaber-Gordon et al., Nature **391**, 156 (1998)
- [2] D. Goldhaber-Gordon et al., Physical Review Letters **81**, 5225 (1998)
- [3] J. Göres et al., Phys. Rev B **62**, 2188 (2000)
- [4] Y. R. D. Mahalu and H. Shtrikman, Phys. Rev. Lett. **88**, 076601 (2002)
- [5] M. Sato et al.; Phys. Rev. Lett. **95**, 066801 (2005)
- [6] R. Scheibner et al., Phys. Rev. Lett. **95**, 176602 (2005)
- [7] T. Kim and S. Hershfield, Phys. Rev. Lett. **88**, 136601 (2002)
- [8] T. Kim and S. Hershfield, Phys. Rev. B **67**, 165313 (2003)
- [9] W. Hofstetter *et al.*, Phys. Rev. Lett. **87**, 156803 (2001)
- [10] K.G. Wilson, Rev. Mod. Phys. **47**, 773 (1975); H. R. Krishna-murthy, J. W. Wilkins and K. G. Wilson, Phys. Rev. B **21**, 1003 (1980).
- [11] M. Yoshida, M. A. Whitaker, L.N. Oliveira, Phys. Rev. B **41**, 9403 (1990)
- [12] V.L. Campo Jr and L.N. Oliveira, Phys. Rev. B **72**, 104432 (2005)
- [13] J.M. Ziman, Principles of The Theory of Solids, Cambridge University Press 1972
- [14] B.R. Bulka and P. Stefański, Phys. Rev. Lett. **86**, 5128 (2001)
- [15] W.C. Oliveira and L.N. Oliveira, Phys. Rev. B **49**, 11986 (1994)
- [16] S.C. Costa, C.A. Paula , V. L. Lbero and L.N. Oliveira, Phys. Rev. B **55** 30 (1997)